

In Press, Accepted Manuscript – Note to user

Numerical Analysis of the ZnGeN₂ Layer Effect on InGaN/GaN Multiple Quantum Well Light-Emitting Diodes.

Laznek Samira ^{a*}, Messei Nadia ^b, and Abdallah Attaf ^b

^a Department of SM, Faculty of Exact, Natural and Life Science, Mohamed Khider University, Biskra 07000, Algeria.

^b Laboratory of Thin Films and Applications, Mohamed Khider University, Biskra 07000, Algeria.

*Corresponding author. Tel.: +213-793-73-06-79; e-mail: samira.laznek@univ-biskra.dz

Received 31 March 2023, Revised 27 July 2023, Accepted 17 August 2023

ABSTRACT

This paper discusses the effect of a ZnGeN₂ layer inserted into the wells of Type-I InGaN/GaN QWs LEDs on the electrical and optical properties by using Silvaco TCAD Simulator. First, the new structure is compared to standard type-I LED based on InGaN. We found that using ZnGeN₂ layer in the In_{0.2}Ga_{0.8}N-QWs LED leads to wavelength extending from the blue to the red region. Next, we highlighted the effect of quantum well number and In-molar fraction in the wells of In_xGa_{1-x}N/ZnGeN₂ type-II LEDs. As a result, increasing the number of wells from two to six QWs creates spontaneous emissions beyond 530 nm while maintaining a low concentration of indium in the wells ($x = 0.16$) and improving the electrical and optical properties, as we found an improvement in light output power of 10.7% at 40Acm⁻².

Keywords: ZnGeN₂, band offset, Silvaco TCAD simulator, type-II, QWs

1. INTRODUCTION

In recent years, white-colored light-emitting diodes (LEDs) have received a lot of attention due to their enormous potential for energy-saving in general lighting applications [1-3]. They have been generally fabricated by using InGaN/GaN quantum wells. GaN can exhibit emission over the full visible range due to wide energy band, which changes by adjusting the composition of the alloy [4, 5]. The use of high In-content in InGaN/GaN LEDs QWs to broaden the emission band of the green and especially red wavelength leads to large piezoelectric and spontaneous polarization fields that greatly affect the efficiency reduction [6]. For this reason, several studies proposed an effective solution to improve efficiency by using the type-II InGaN/ZnGeN₂ in the active region of QWs LEDs.

New promising semiconducting materials with large and direct gap have emerged as the zinc germanium nitride ZnGeN₂. Band offsets at heterojunction play an important role in previous semiconductor devices. The strong confinement of holes in the ZnGeN₂ layer resulting from high valence band offset allows broadening of the emission into the red wavelength by using a lower In-content in the type-II InGaN/ZnGeN₂ QWs structure [7, 8]. Some studies have determined the valence band offset between ZnGeN₂ and GaN using x-ray photoemission spectroscopy that is 1.45–1.65 eV above that of GaN [9].

The zinc germanium nitride ZnGeN₂ have characteristics very close to GaN where the lattice mismatch between them is less than 1%. The experimental lattice parameters

for ZnGeN₂ are $a = 3.1962 \text{ \AA}$ and $c = 5.2162 \text{ \AA}$ with those for GaN ($a = 3.185 \text{ \AA}$ and $c = 5.18 \text{ \AA}$) [10]. In addition, the band gap of Zn-IV-N₂ materials covers a wide range of wavelengths ranging from infrared to ultraviolet, just like III-V materials, and is therefore remarkable for light-emitting devices [10]. The values for the spontaneous and piezoelectric polarizations also indicate that these materials will cause fewer problems than their III-V analogs for example the Stark effect [10].

Many search groups have been studied the type-II QW structures to improve the optical and electrical proprieties of the InGaN/GaN QW structure. Among these type-II QW structures are the type-II InGaN/ZnSnN₂/GaN heterostructure and the type-II InGaN/GaN_{0.9}Sb_{0.1}/GaN heterostructure [11, 12]. InGaN and ZnGeN₂ materials have structural and optical properties compatible and those to those of III-V elements [10]. Therefore, appear to be reasonable to realize the type-II InGaN/ZnGeN₂ heterostructure and to insert a thin layer of ZnGeN₂ into the active region of InGaN standard LEDs. On other hand, the type -II InGaN/ZnGa_{0.9}N_{0.1}/InGaN QW structure was proposed to obtain LEDs light emitting of longer wavelength typically beyond 530 nm with a high efficiency, while keeping a low concentration of indium in the wells.

In this work, we study the effect of quantum well number and the In-molar fraction on the electronic and optical properties of the type-II QWs LED structure combining InGaN and ZnGeN₂. To simulate the nanoscale effects in the QWs and their impact on device performance, we used SILVACO simulation software. SILVACO/ TCAD uses the self-consistent 6-band Luttinger-Kohn k.p model to

calculate band structures, which takes into account for voltage effects, offset of valence bands and polarizations spontaneous and piezoelectric. Shockley–Read–Hall recombination and Auger non-radiative recombination mechanisms are also taken into account. Iteratively solving the Schrodinger and Poisson equations gives a description quantum of bound energy states in the quantum well with changing device bias and the use a free carrier model is to calculate spontaneous photon emission [13-17]. Nevertheless, the drift-diffusion model alone does not reflect the actual behavior of charge carriers in the quantum wells and barriers. Indeed, this model assumes that the bound carriers of the well are in equilibrium with the carriers of the bulk layers and makes no difference between them [18]. For this reason, a new model was developed by SILVACO [18, 19]. The capture-escape model, allows tracking dynamics of bound carriers in quantum wells. It also allows accounting for the effect of quantum charge by including it self-consistently in the Poisson equation.

2. DEVICE STRUCTURE

In this study, we used two devices model with a rectangular chip size of 200x200 μm . One is a conventional LED emitting light blue whose architecture is illustrated in figure 1a, and the second has the same structure, with layers of ZnGeN₂ 1nm thick added inside the quantum wells as shown in figure 1b. This LEDs structure has a 200 nm thick p- GaN layer (Si: 10¹⁹ cm⁻³), followed by an electron blocking layer (EBL) to reduce the electron-hole recombination at the p-side with AlGaN with 15% aluminum for a 45 nm thick (10¹⁹ cm⁻³), active zone composed of 2 quantum wells of InGaN at 20% indium 3 nm thick separated by undoped layers 6 nm thick GaN barriers finally 3 μm thick n- GaN layer (Mg:10¹⁸ cm⁻³). The

In_xGa_{1-x}N gap energy variation with fraction molar of indium and material parameters to be used for the proposed structure is shown in the two equations (1), (2) and in table 1.

The In_xGa_{1-x}N energy gap was evaluated from GaN and InN Vegard's law:

$$E_g(\text{In}_x\text{Ga}_{1-x}\text{N}) = xE_g(\text{InN}) + (1-x)E_g(\text{GaN}) - 1.43x(1-x) \quad (1)$$

The Varshni law evaluated the variation of energy gap with temperature [20, 21]:

$$E_g(T) = E_g(0) - \delta T^2 / \gamma + T \quad (2)$$

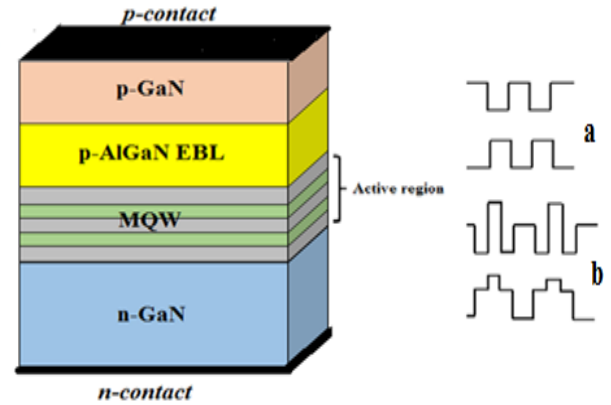


Figure 1. Schematic diagram of the LED structure investigated with 2-QW in the active region for (a) type-I GaN-InGaN-GaN and (b) type-II GaN-InGaN-ZnGeN₂-InGaN-GaN.

Table 1 Material parameters used in SILVACO at 300K [22, 23]

Material parameters	In _{0.2} Ga _{0.8} N	GaN	InN
$E_g(0)$ (eV)	2.64	3.42	0.7
γ (eV/k)	6.6 x10 ⁻⁴	9.9 x10 ⁻⁴	2.45 x10 ⁻⁴
δ (k)	755	830	-
Hole lifetime τ_p (s)	10 ⁻⁹	10 ⁻⁹	-
Electron lifetime τ_n (s)	10 ⁻⁹	10 ⁻⁹	-
Electron Auger coefficient AUG_n (s)	10 ⁻³⁴	10 ⁻³⁴	-
Hole Auger coefficient AUG_p (s)	10 ⁻³⁴	10 ⁻³⁴	-
Radiative recombination rate constant COPT (s)	1.1 x10 ⁻⁸	1.1 x10 ⁻⁸	-
Electron Recombination Shockley-Read-Hall SRH. τ_n (s)	2x10 ⁻⁷	2x10 ⁻⁷	-
Hole Recombination Shockley-Read-Hall SRH. τ_p (s)	2x10 ⁻⁷	2x10 ⁻⁷	-

3. RESULTS AND DISCUSSION

3.1. Energy Band Alignment

Figure 2 shows potential energy profiles where figure 2a is for the type-I GaN/In_{0.2}Ga_{0.8}N/GaN and figure 2b is for the type-II In_{0.2}Ga_{0.8}N/ZnGeN₂/ In_{0.2}Ga_{0.8}N QWs LED structure at 40 A/cm². The wave functions of electrons (Ψ_{e1}) and holes (Ψ_{hh1}) in two quantum wells are also shown, 1e correspond to the first conduction band excited levels and 1hh at valence band excited levels heavy holes. The well

width of the type-I and type-II QWs structure is fixed as $L_w = 3$ nm. The transitions between the 1e and 1hh energy levels E_{g1-hh1} is responsible for spontaneous emission peaks. Thus, the position of the spontaneous emission peak is entirely determined by the position of the 1e and 1hh energy levels and this explain the change in spontaneous emission peak when inserting the ZnGeN₂ layer as it will lead to a significant shift in the energy levels and a shift in the spontaneous emission of the LED. In addition, an overlap exists between the functions of electron and hole wave functions in the two wells, this will lead to an a

increase in the radiative recombination as shown in figure 2c.

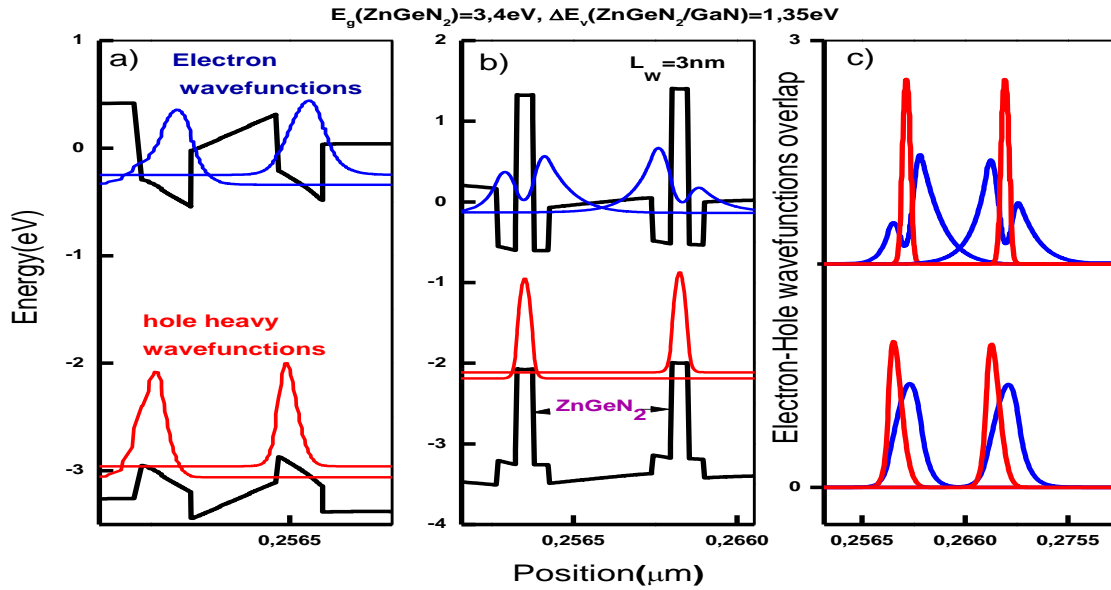


Figure 2. Potential energy profiles for (a) type-I GaN/In_{0.2}Ga_{0.8}N/GaN QWs, (b) type-II In_{0.2}Ga_{0.8}N/ZnGeN₂/In_{0.2}Ga_{0.8}N QWs at 40A/cm². Ψ_{e1} and Ψ_{hh1} are also shown as blue and red lines, respectively and figure (c) electron-hole wavefunctions overlap.

3.2. Comparison of Spontaneous Emission for the Conventional type-I and the type-II In_{0.2}Ga_{0.8}N/ZnGeN₂/In_{0.2}Ga_{0.8}N QWs LED structure.

Figure 3, compares the spontaneous emission of the conventional type-I GaN/In_{0.2}Ga_{0.8}N/GaN QWs with the type-II In_{0.2}Ga_{0.8}N/ZnGeN₂/In_{0.2}Ga_{0.8}N QWs LED structure according to various injection current densities 10, 20 and 40A/cm². Figure 3 shows a significant enhancement of the spontaneous emission peaks of the type-II QWs

compared to the conventional type-I QWs LED structure. As shown in Figure 3, the use of the ZnGeN₂ layer in the InGaN-QW extends the wavelength from the blue $\lambda = 455$ nm to the red region $\lambda = 609$ nm. The next step is modifying other parameters such as the indium molar fraction and the quantum well number and studying their effect on the optical and electrical properties to achieve the performance of these LEDs.

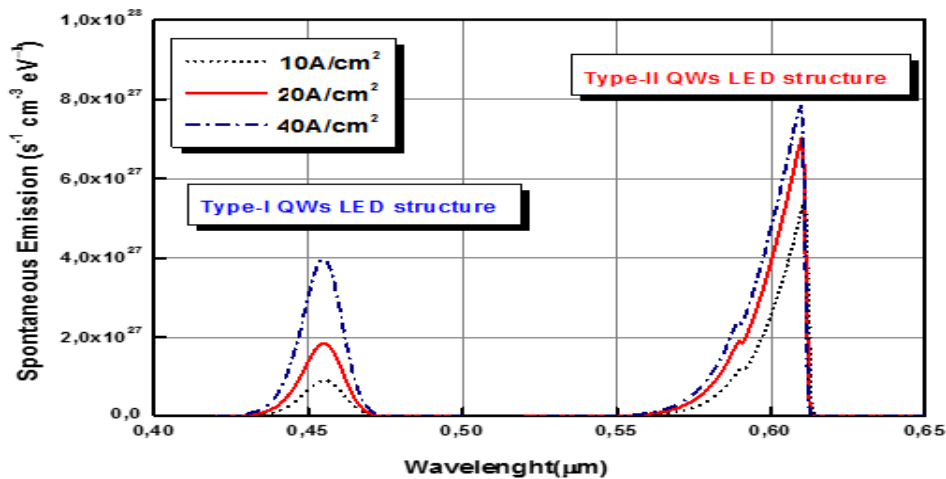


Figure 3. Spontaneous emission spectra on function of wavelength for type-I and type-II QWs LED structures at various injection current density.

3.3. Effect of Injection Current Density in the Spontaneous Emission of type-II $\text{In}_{0.2}\text{Ga}_{0.8}\text{N}/\text{ZnGeN}_2$ QWs LED Structure.

We investigated the effect of injection current density in the spontaneous emission of the type-II $\text{In}_{0.2}\text{Ga}_{0.8}\text{N}/\text{ZnGeN}_2/\text{In}_{0.2}\text{Ga}_{0.8}\text{N}$ QWs LED structure. Figure 4 shows the effect of injection current density on

conduction and valence band, a negligible change in conduction and valence band at current densities 10, 20 and 40 A/cm^2 , whereas, at 60, 80 and 100 A/cm^2 we observe a large change, which leads to a direct modification in energy levels, wavelengths and spontaneous emission. Simulation results are shown in table 2 and figure 5.

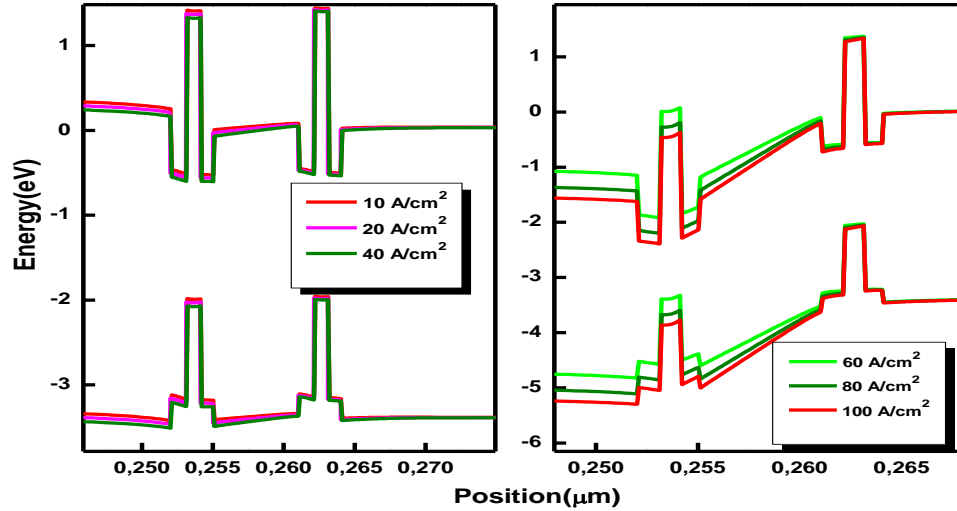


Figure 4. Potential energy profiles of the type-II $\text{In}_{0.2}\text{Ga}_{0.8}\text{N}/\text{ZnGeN}_2/\text{In}_{0.2}\text{Ga}_{0.8}\text{N}$ QWs LED structure as a function of versus injection current density.

Table 2 Effect of injection current density in wavelengths and spontaneous emission of the type-II $\text{In}_{0.2}\text{Ga}_{0.8}\text{N}/\text{ZnGeN}_2/\text{In}_{0.2}\text{Ga}_{0.8}\text{N}$ QWs LED structure.

Injection current (A/cm^2)	Peak energy (eV)	λ (nm)	Spontaneous emission ($\text{s}^{-1} \text{cm}^{-3} \text{eV}^{-1}$)
10	2.032	610	5.30×10^{27}
20	2.032	610	7.10×10^{27}
40	2.032	611	7.86×10^{27}
60	1.962	632	2.02×10^{27}
80	1.937	640	2.21×10^{27}
100	1.919	646	2.53×10^{27}

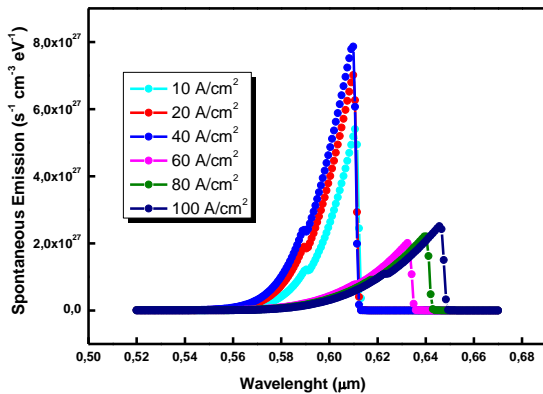


Figure 5. Spontaneous emission spectra of the type-II $\text{In}_{0.2}\text{Ga}_{0.8}\text{N}/\text{ZnGeN}_2/\text{In}_{0.2}\text{Ga}_{0.8}\text{N}$ QWs LED structure as a function of versus injection current density.

Figure 6 shows peaks of spontaneous emission as a function of current density for type-II $\text{In}_x\text{Ga}_{1-x}\text{N}/\text{ZnGeN}_2$ QWs structures with Indium content changed from $x=0.16$ to 0.20. Moreover, we observe that the type-II $\text{In}_x\text{Ga}_{1-x}\text{N}/\text{ZnGeN}_2$ QWs structure have much larger spontaneous emission peaks for lower Indium content as a function of current density. On the other hand, the type-II $\text{In}_x\text{Ga}_{1-x}\text{N}/\text{ZnGeN}_2$ QWs LED structure ($x = 0.2$) have smaller spontaneous emission peaks compared to QWs structure with an Indium content equal to 0.16 and 0.18. The greatest value is observed at 40 A/cm^2 is $7.86 \times 10^{27} \text{ s}^{-1} \text{cm}^{-3} \text{eV}^{-1}$. After this value, a decrease is observed because the modification of the conduction and the valence band leads to a modification of the energy levels and a spontaneous

emission. We conclude that the best spontaneous emission peak for QWs $\text{In}_x\text{Ga}_{1-x}\text{N}/\text{ZnGeN}_2$ type-II structures is at indium content equal to $x=0.16$.

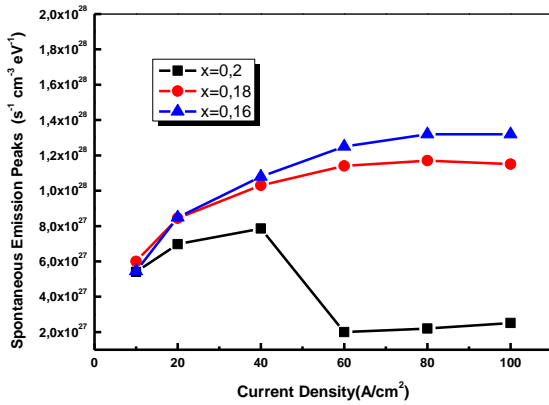


Figure 6. Peaks spontaneous emission of the type-II $\text{In}_x\text{Ga}_{1-x}\text{N}/\text{ZnGeN}_2$ QWs LED structure as a function of current density with Indium content: $x=0.16, 0.18$ and 0.20

3.4. Effect of In-Molar Fraction (x) on the Electrical and Optical Characteristics of the type-II $\text{In}_x\text{Ga}_{1-x}\text{N}/\text{ZnGeN}_2/ \text{In}_x\text{Ga}_{1-x}\text{N}$ QWs LED structure.

The injection current density versus forward voltage of different In-molar fraction is simulated in both quantum wells layers as illustrated in figure 7. In the type-II $\text{InGaN}/\text{ZnGeN}_2$ QWs LED structure, the anode current decreases when the In-molar fraction increases in quantum wells. The best current density is of $115.98 \text{ A}/\text{cm}^2$ for $x=0.16$. There a slight impact on EQE and light output power in the lower injection current and under higher injection current density the efficiency droop is increased as the In-molar fraction in the two wells increases, with can be clearly seen in the figure 8a. At density of constant current, it is a decreasing function of the increasing In-molar fraction. Therefore, at $40 \text{ A}/\text{cm}^2$, the luminous output powers of the structures are respectively equal to 15.46 mW , 15.16 mW , and 14.24 mW shown in figure 8b. As for spontaneous emission. We can see in the figure 9, an increase in molar fraction in the two wells leads a broadening of the wavelengths with decrease in spontaneous emission peak.

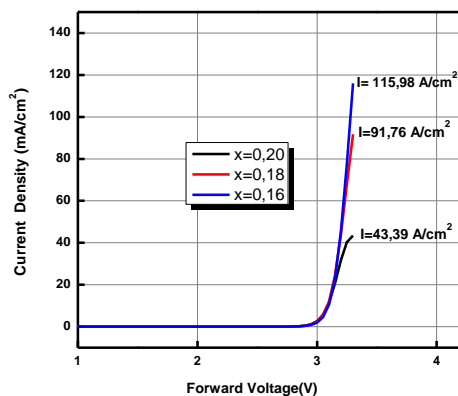


Figure 7. The injection current density versus forward voltage of the type-II $\text{In}_x\text{Ga}_{1-x}\text{N}/\text{ZnGeN}_2$ QWs LED structure as a function for various molar fraction x .

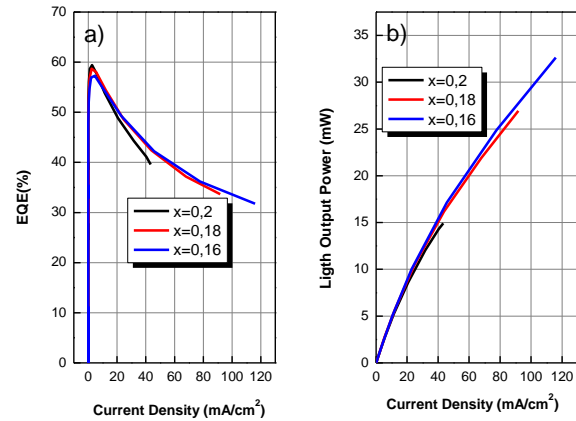


Figure 8. External quantum efficiency and Light Output Power of the type-II $\text{In}_x\text{Ga}_{1-x}\text{N}/\text{ZnGeN}_2$ QWs LED structure as a function for various molar fraction x .

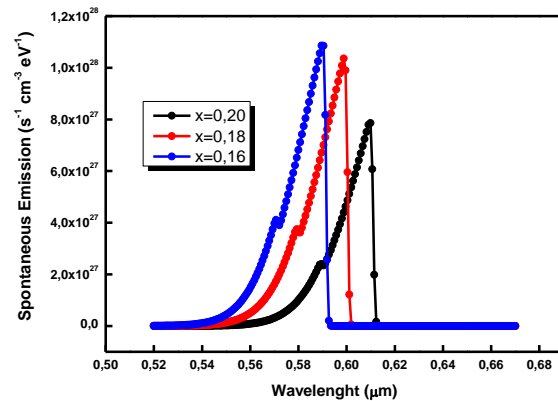


Figure 9. Spontaneous emission spectra of the type-II $\text{In}_x\text{Ga}_{1-x}\text{N}/\text{ZnGeN}_2$ QWs LED structure as a function for various molar fraction x .

3.5. Effect of Quantum Well Number in the Optical and Electrical Characteristics of type-II $\text{In}_{0.16}\text{Ga}_{0.84}\text{N}/\text{ZnGeN}_2$ QWs LED Structure.

Simulated concentration of electrons and holes in the active region of type-II $\text{In}_{0.16}\text{Ga}_{0.84}\text{N}/\text{ZnGeN}_2$ 2-4-6 QWs and the potential energy profile of the type-II 6-QWs structure of LED shows in the figure 10 a d and in the figure 10 c, respectively under injection current density $40 \text{ A}/\text{cm}^2$. When the QW number increases from 2 to 6, the results indicate that with a large number of quantum well, the electrons and holes will be distributed more uniformly and will be more concentrated to the quantum wells, with different electron concentrations in each well, where we observe two very distinct peaks on either side of the ZnGeN_2 layer. Even the holes, their concentrations and

distribution increases better in the ZnGeN₂ regions with the increasing quantum well number.

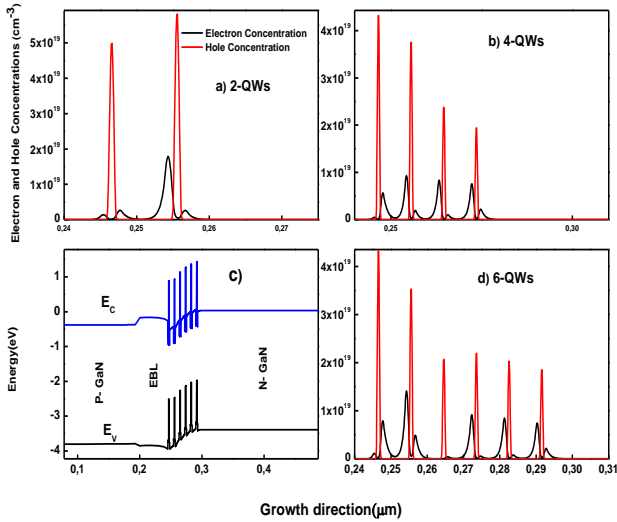


Figure 10. The concentration of electrons and holes in the active regions of type-II In_{0.16}Ga_{0.84}N/ZnGeN₂ QWs LED structure, (a) 2-QWs, (b) 4-QWs, (d) 6-QWs and (c) the potential energy profile of the type-II 6-QWs structure under injection current density 40 A/cm².

Figure 11 show the injection current density versus forward voltage of the type-II In_{0.16}Ga_{0.84}N/ZnGeN₂ QWs LED structure with increasing number of quantum well simulated. The forward voltage at 40A/cm² decreases from 3.7 V to 3.19 as the quantum well number decreases from six to four and two respectively.

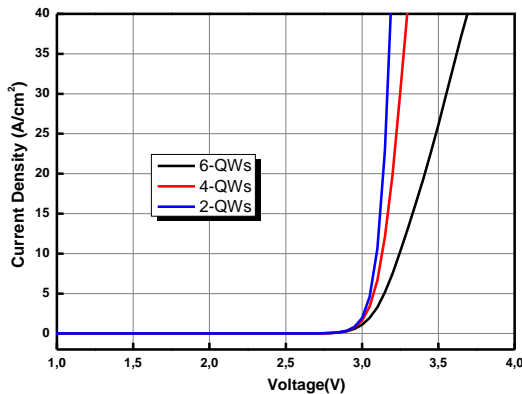


Figure 11. The Injection current density versus forward voltage of the type-II In_{0.16}Ga_{0.84}N/ZnGeN₂ QWs LED structure as a function for various number of QW.

To determine the effects of the quantum well number on the optical power and the efficiency all parameters are kept constant including SRH lifetime as first step. Figure 12 shows the computed EQE and light output power with increasing current density for the LEDs of varying QW number. The simulated optical output power from the LEDs with 2, 4 and 6 QWs was measured, as presented in

figure 12.b. It shows that the output power of 2, 4 and 6 - QWs LEDs is 15.46, 16.86 and 17.30 mW, respectively, at the current density of 40 A/cm². The numerical optical output power is increased with 10.70 % when the QW number increases from 2 to 6.

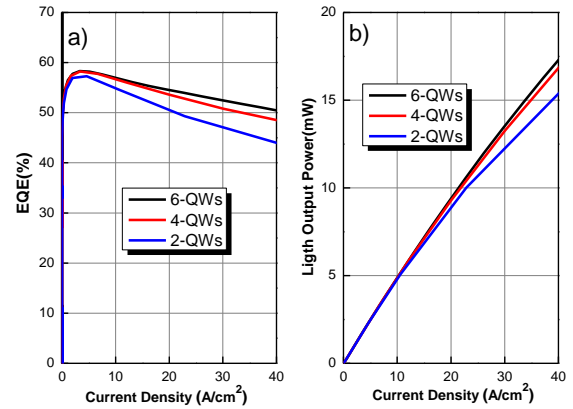


Figure 12. External quantum efficiency and Light Output Power of the type-II In_{0.16}Ga_{0.84}N/ZnGeN₂ QWs LED structure as a function for various number of QW.

When the QW number increases, we can see in the figure 12 a. b the enhancement on the light output power and EQE at all current density levels and this enhancement become increasingly apparent under higher injection current density. On other hand, the efficiency loss (droop) reducing with increasing the number of QW. To explain this change on the EQE, radiative recombination rates are calculated (SRH and Auger) at 40 A/cm² and depicted in figure 13 a, 13 b and 13 c. All rates are distributed more significantly in the LED 2-QWs structure; the concentration these rates in the second well and slightly lower for the first well. For the structure with four quantum wells, the rates radiative recombination, SRH and Auger shifts for the first two QWs, and remains equal for the last two quantum wells.

As for the last structure, which consists of 6-QWs, the radiative recombination rate, SRH and Auger are equally distributed amongst the six wells, which can be clearly seen in the figure 13 a b c. In the ZnGeN₂ layers, Auger and SRH recombination equals to zero, for 2-4-6 QWs LEDs because of the absence of electrons concentration as shown in figure 13 a b c.

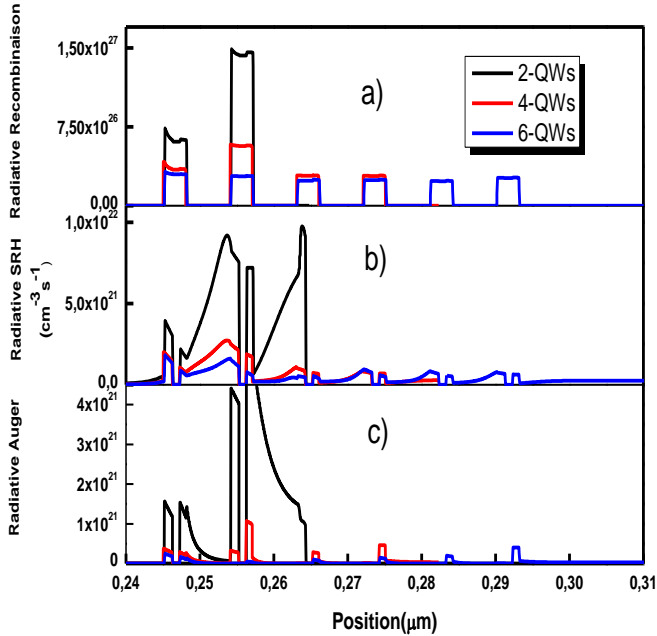


Figure 13. The rates of (a) radiative recombination, (b) SRH and (c) Auger at 40 A/cm² of the type-II In_{0.16}Ga_{0.84}N /ZnGeN₂ QWs LED structure.

The type-II InGaN/ZnGeN₂ 2-QWs structure show a significant efficiency loss compared to that for the type-II 4-QWs and the type-II 6-QWs structure at high-injected current densities, this efficiency droop is result from a higher value of Auger recombination by electron-phonon coupling, as this phenomenon originates from the excitation of the Auger recombination and it have been demonstrated experimentally by J. Iveland et al [24-26].

Figure 14 and table 3 show the effect of increasing the number of wells in the active region on both the wavelength and the spontaneous emission. When increasing the number of wells the wavelength extends from $\lambda=589$ nm to the $\lambda=598$ nm, this change is accompanied by a decrease in the spontaneous emission peak.

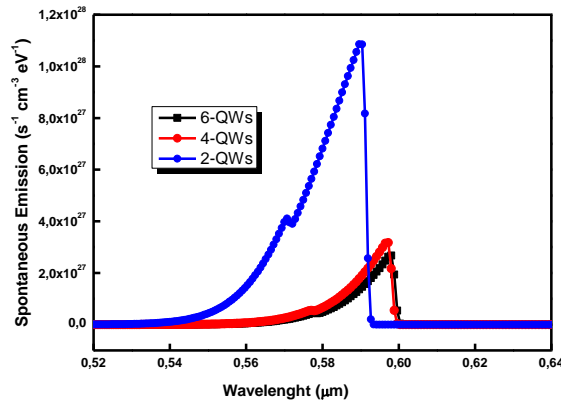


Figure 14. Spontaneous emission for the type-II In_{0.16}Ga_{0.84}N /ZnGeN₂ QWs LED structure as a function for various number of QW.

Table 3 Effect number of quantum well in wavelengths and spontaneous emission for the type-II In_{0.16}Ga_{0.84}N /ZnGeN₂ QWs LED structure.

Number of wells	Peak energy (eV)	λ (nm)	Spontaneous emission (s ⁻¹ cm ⁻³ eV ⁻¹)
2-QWs	2.105	589	1.08 x10 ²⁸
4-QWs	2.080	596	3.21 x10 ²⁷
6-QWs	2.073	598	2.73 x10 ²⁷

4. CONCLUSION

The electronic and optical properties of type-II InGaN/ZnGeN₂-QWs LEDs structure have been investigated by using the Silvaco TCAD simulator. The ZnGeN₂ layers inserted in InGaN/GaN QWs active region allow electron-hole wave function overlap by strongly confining the hole wave function in the ZnGeN₂ layers due to the large valence band offset. The conduction band offset between InGaN and ZnGeN₂ creates very distinct peaks on both sides of the ZnGeN₂ layer which affected the energy levels and overlap between of electron-hole wave functions. As a result, the wavelength and the spontaneous emission peak intensity improve compared to the standard InGaN QWs LED. In this work, we have discussed the effect of the In-molar fraction in type-II In_xGa_{1-x}N/ZnGeN₂-QWs LED, where we have found a slight effect on the optical and electrical characteristics with an extension of the wavelength. Moreover, we have observed that the use of a high indium content ($x = 0.2$) in the type-II InGaN/ZnGeN₂-QWs LED structure for an injection current density greater than 40 A cm⁻² leads to a modification significant potential energy profiles, which is reflected in both wavelengths and spontaneous emission, as it extends emission into regions with longer wavelengths. Finally, the use of MQWs of the type-II InGaN/ZnGeN₂-QWs in LED devices is discussed. So, we propose this later as an effective way to increase the emission wavelength of the LEDs, keeping a low concentration of indium in the wells ($x=0.16$).

REFERENCES

- [1] Velpula, R. T. Jain, B. Bui, H. Q. T. Shakiba, F. M. Jude, J. Tumuna, M. Nguyen, H. -D. Lenka, T. R. and Nguyen, H. P. T. (2020). Improving carrier transport in AlGaIn deep-ultraviolet light-emitting diodes using a strip-in-a-barrier structure. *Applied Optics*. Volume: 59 Issue: 17. 5272 – 5281.
- [2] Jain, B. Velpula, R. T. Bui, H. Q. T. Nguyen, H.-D. Lenka, T. R. Nguyen, T. K. and Nguyen, H. P. T. (2020). High performance electron blocking layer-free InGaIn/GaN nanowire white-light-emitting diodes. *Optics Express*. Volume: 28 Issue: 1. 665 – 675.
- [3] Chen, Y. Haller, C. Liu. W. Karpov, S. Y. Carlin, J. -F. and Grandjean, N. (2021). GaN buffer growth temperature and efficiency of InGaIn/GaN quantum wells: the critical role of nitrogen vacancies at the GaN surface. *Applied Physics Letters*. Volume: 118 Issue: 11. 111102.
- [4] Araki, T. Saito, Y. Yamaguchi, T. Kurouchi, M. Nanishi, Y. and Naoi, H. (2004). Radio frequency-molecular beam epitaxial growth of InN epitaxial films on (0001) sapphire and their properties. *J. Vac. Sci. Technol. B*. Volume: 22 Issue: 4. 2139–2143.
- [5] Brunner, D. Angerer, H. Bustarret, E. Freudenberg, F. Höppler, R. Dimitrov, R. Ambacher, O. and Stutzmann, M. (1997). Optical constants of epitaxial AlGaIn films and their temperature dependence. *Journal of Applied Physics*. Volume: 82 Issue: 10. 5090 – 5096.
- [6] Zhou, Q. Xu, M. and Wang, H. (2016). Internal quantum efficiency improvement of InGaIn/GaN multiple quantum well green light-emitting diodes. *Journal Opto-Electronics Review*. Volume: 24 Issue: 1. 1 – 9.
- [7] Han, L. Kash, K. and Zhao, H. (2016). Designs of blue and green light-emitting diodes based on type-II InGaIn-ZnGeN₂ quantum wells. *Journal of Applied Physics*. Volume: 120 Issue: 10. 103102.
- [8] Hyot, B. Rollès, M. and Miska, P. (2019). Design of Efficient Type-II ZnGeN₂/In_{0.16}Ga_{0.84}N Quantum Well-Based Red LEDs. *Rapid Research Letter*. Volume: 13 Issue: 8. 1900170.
- [9] Karim, M. R. Noesges, B. A. Jayatunga, B. H. D. Zhu, M. Hwang, J. Lambrecht, W. R. L. Brillson, L. J. Kash, K. and Zhao, H. (2021). Experimental determination of the valence band offsets of ZnGeN₂ and (ZnGe)_{0.94}Ga_{0.12}N₂ with GaN. *J. Phys. D: Appl. Phys*. Volume: 54 Issue: 24. 245102.
- [10] Tellekamp, M. B. Miller, M. K. Rice, A. D. and Tamboli, A. C. (2016). Heteroepitaxial ZnGeN₂ on AlN: Growth, Structure, and Optical Properties. *Cryst. Growth Des*. Volume: 22 Issue: 2. 1270-1275.
- [11] Arif, R. A. Zhoa, H. and Tansu, N. (2008). Type-II InGaIn-GaNAs quantum wells for lasers applications. *Applied Physics Letters*. Volume: 92 Issue: 1. 011104.
- [12] Karim, M. R. and Zhao, H. (2018). Design of InGaIn-ZnSnN₂ quantum wells for high-efficiency amber light emitting diodes. *Journal of Applied Physics*. Volume: 124 Issue: 3. 034303.
- [13] Kioupakis, E. Yan, Q. and Van de Walle, C. G. (2012). Interplay of polarization fields and Auger recombination in the efficiency droop of nitride light-emitting diodes. *Applied Physics Letters*. Volume: 101 Issue: 23. 231107.
- [14] Filoche, M. Piccardo, M. Wu, Y. R. Li, C. K. Weisbuch, C. and Mayboroda, S. (2017). Localization landscape theory of disorder in semiconductors. I. Theory and modeling. *Phys. Rev. B*. Volume: 95 Issue: 14. 144204.
- [15] Li, C. K. Piccardo, M. Lu, L. S. Mayboroda, S. Martinelli, L. Peretti, J. Speck, J. S. Weisbuch, C. Filoche, M. and Wu, Y. R. (2017). Localization landscape theory of disorder in semiconductors. III. Application to carrier transport and recombination in light emitting diodes. *Phys. Rev. B*. Volume: 95 Issue: 14. 144206.
- [16] Mounir, C. Schwarz, U. T. Koslow, I. L. Kneissl, M. Wernicke, T. Schimpke, T. and Strassburg, M. (2016). Impact of inhomogeneous broadening on optical polarization of high-inclination semipolar and nonpolar In_xGa_{1-x}N/GaN quantum wells. *Phys. Rev. B*. Volume: 93 Issue: 23. 235314.
- [17] Auf der Maur, M. Galler, B. Pietzonka, I. Strassburg, M. Lugauer, H. and Carlo, A. D. (2014). Trap-assisted tunneling in InGaIn/GaN single-quantum-well light-emitting diodes. *Appl. Phys. Lett*. Volume: 105 Issue: 13. 133504.

- [18] SILVACO. (2016). Atlas User's Manual. SILVACO: Santa Carla, CA, USA. 6-13.
- [19] SILVACO. (2015). ATLAS User's Manual, Device Simulation Software. SILVACO: Santa Carla, CA, USA. 6-254.
- [20] Moses, P. G .and Van de Walle, C. G. (2010). Band bowing and band alignment in InGaN alloys. *Applied Physics Letters*. Volume: 96 Issue: 2. 021908.
- [21] Lang, J. R. Young, N. G. Farrell, R. M. Wu, Y.-R. and Speck, J. S. (2012). Carrier escape mechanism dependence on barrier thickness and temperature in InGaN quantum well solar cells. *Applied Physics Letters*. Volume: 101 Issue: 18. 181105.
- [22] Wu, J. Walukiewicz, W. Yu, K. M. Ager III. J. W. Haller, E. E. Hai, L. and Schaff, W. J. (2002). Small band gap bowing in $\text{In}_x\text{Ga}_{1-x}\text{N}$ alloys. *Appl. Phys. Lett.* Volume: 80 Issue: 25. 4741-4743.
- [23] Wu, J. and Walukiewicz, W. (2003). Band gaps of InN and group III nitride alloys. *Superlattices and Microstructures*. Volume: 34 Issue: 1-2. 63-75.
- [24] Verzellesi, G. Saguatti, D. Meneghini, M. Bertazzi, F. Goano, M. Meneghesso, G. and Zanoni, E. (2013). Efficiency droop in InGaN/GaN blue light-emitting diodes: Physical mechanisms and remedies. *Journal of Applied Physics*. Volume: 114 Issue: 7. 071101.
- [25] Iveland, J. Martinelli, L. Peretti, J. Speck, J. S. and Weisbuch, C. (2013). Direct Measurement of Auger Electrons Emitted from a Semiconductor Light-Emitting Diode under Electrical Injection: Identification of the Dominant Mechanism for Efficiency Droop. *Phys. Rev. Lett.* . Volume: 110 Issue: 17. 177406.
- [26] Kioupakis, E. Rinke, P. Delaney, K. T. and Van de Walle, C. G. (2011). Indirect Auger recombination as a cause of efficiency droop in nitride light-emitting diodes. *Appl. Phys. Lett.* Volume: 98 Issue: 16. 161107.